A Single-Channel Non-Orthogonal I/Q RF Sensor for Non-Contact Monitoring of Vital Signs

Hongrui Bo [1], Lisheng Xu [1], Liling Hao [1], Yuanzhu Dou [2], Lei Zhao [3], and Wenhua Yu [3]

[1] Department of Electrical Engineering, Sino-Dutch Biomedical and Information Engineering School
Northeastern University, Shenyang, Liaoning Province, 110819, China
xuls@bmie.neu.edu.cn

[2] XIKANG ALPS Technology Co. Ltd.
Shenyang, Liaoning Province, 110179, China

[3] Center for Computational Science and Engineering
School of Mathematics and Statistics, Jiangsu Normal University, Xuzhou, China

Abstract ─ In order to remotely monitor the activities of heartbeat, respiration and body movement, this article designed and implemented a single-channel non-orthogonal in-phase/quadrature (I/Q) RF sensor, which works at the central frequency of 2.4 *GHz*. The designed RF sensor is based on a printed circuit board (PCB) antenna. Taking into account low cost, simple structure and easy fabrication, the antenna is designed and implemented with a special broad-band microstrip-to-coplanar strip line Balun structure by combining the transmitter with the receiver on a PCB to form one single antenna system. The gain of the sensor is 7.7 *dB*. The return loss is -22.7 *dB* at 2.4 *GHz* and the directionality of the antenna is satisfactory for monitoring vital signs. It has been validated that the designed sensor can detect the respiration, heartbeat and body movement accurately in comparison with the signals acquired by respiration sensor and pulse sensor.

Index Terms ─ Non-contact RF sensor, non-orthogonal I/Q signals, vital signs monitoring, Yagi antenna.

I. INTRODUCTION

The cost in healthcare is an important portion of each government's budget, and it is increasing rapidly every year. In America, it is estimated that one hundred million Americans suffer from chronic diseases including heart diseases, lung disorders, and diabetes. The expense for these conditions accounts for three-fourths of total US healthcare expense [1]. If there is a way that the diseases can be prevented at early stage, the costs of healthcare will be significantly reduced. With the advent of big data era, daily vital signs become essential for prevention and diagnosis of diseases. By analyzing daily physiological parameters, doctors are able to diagnose the illness accurately. Monitoring sleep information of infants can reduce the mortality of sudden infant death syndrome (SIDS) [2]. Consequently, there is a growing market for application, which allows monitoring vital signs for convenience and at low cost [3].

Although most of the wearable devices can detect our daily physiological parameters, it is not convenience for our daily life and has low accuracy. Furthermore, most people may be shameful to wear equipment every day [4].

Therefore, there is a great demand for monitoring physiological parameters conveniently with low costs in our daily lives [5-6]. Since the 1970s, microwave Doppler radar has drawn attention for new applications in human healthcare because it offers a non-contact alternative for healthcare monitoring, such as physiologic movement, volume change sensing [7], life detection for finding human subjects trapped in earthquake rubble [8], and cardiopulmonary monitoring for sleep apnea syndrome detection [9-10], remote non-contact detection of vital signs, and so on.

The respiration and heartbeat, based on microwave Doppler phase modulation technique, has been studied for many years [11]. Nevertheless, Doppler radar used for detecting vital signs has not been commoditized and is still under being investigated. The most important limitation in Doppler radar measurement of periodic motion is the presence of the null demodulation points [12]. When vital signs become weak with a lot of background noise caused by walking and talking of the people nearby, it will be hard for the radar sensor to detect the relative weak vital signs from strong background noise, unless shorter carrier wavelength is used to improve the sensitivity [13]. In consequence, single-channel receiver cannot be used and a multiple antenna system is required, which means this kind of

Submitted On: November 18, 2015
Accepted On: May 3, 2016

Doppler radar system is complex [14-15].

In summary, there is a huge market for a new kind of sensor with simple structure and accurate detection. Compared with Doppler radar, this article analyzes and designs an RF sensor working at the frequency of 2.4 *GHz* for monitoring physiological parameters, which can form a single-antenna system. In principle, our antenna detects body movements by the shift of phases; however Doppler radar detects the body movements by the change of frequency [16]. Therefore, our antenna can form a single-antenna system and provide a more accurate detection method with low noise [17]. Due to the ease production of PCB antenna, our design also ensures the possibility of mass production with low cost.

II. PRINCIPLE OF DETECTING MOTION BY MICROWAVE

According to the principle of microwave, the phase of signal and the location of the time-varying moving target will be modulated in a linear scale and reflected again by a time-varying moving target whose rate close to zero. In comparison with the speed of electromagnetic wave, the speed of human body's breathing almost close to zero in quiet state. Therefore, a microwave radar targets in thoracic will receive the phase modulation signal with time varying movement of thoracic position similar to launch signal. This signal contains information of respiration, heartbeat and body movements. Therefore, the signal of single frequency microwave radars can be expressed as follows:

$$S(t) = A_0\, cos[2\pi f t + \phi(t)], \tag{1}$$

where, A_0 is the amplitude of the transmitted signal; $\phi(t)$ is the phase of the transmitted signal; f is the frequency of the signal.

The total distance that radar signal comes from the transmitting antenna to the receiving antenna is $2d(t) = 2d_0 + 2x(t)$, where d_0 is the distance between the transmitting antenna and the subject, $x(t)$ is the distance caused by thoracic motion. In order to simplify the computation, the amplitude A_0 is equal to 1. Therefore, the echo signal is launched by the body as follows:

$$S_F(t)=cos[2\pi f(t-\frac{2d(t-\frac{d(t)}{c_0})}{c_0})+\phi(t-\frac{2d(t-\frac{d(t)}{c_0})}{c_0})], \tag{2}$$

where, c_0 is the speed of light, the cycle of chest movement caused by respiration is $T \gg \frac{d_0}{c_0}$, so in $x(t-\frac{d(t)}{c_0})$, $\frac{d(t)}{c_0}$ can be neglected. Thus, the received echo signal can be expressed as follows:

$$S_F(t) \approx cos[2\pi f(t-\frac{4\pi d_0}{\lambda}-\frac{4\pi x(t)}{\lambda})+\Phi(t-\frac{2d_0}{c_0})]. \tag{3}$$

Having compared this function with Equation (1), the received radar echo signal is similar with the transmitting signal. The reason is that the phase of the echo signal is modulated by the movement of the thorax, as well as the delay caused by the distance between subject and radar.

Mixing the echo signal with the local oscillator signal results in a conversion directly to baseband signal $BD(t)$:

$$BD(t) = cos(\theta + \frac{4\pi x(t)}{\lambda} + \Delta\phi(t)), \tag{4}$$

where, $\Delta\phi(t) = \phi(t) - \phi\left(t - \frac{2d_0}{c_0}\right)$ is the rest of the phase noise, $\theta = \frac{4\pi d_0}{\lambda} + \theta_0$ is the inherent phase shift, which is determined by d_0. θ_0 is caused by the phase shift of the reflection plane, mixer and the distance between the antennas and so on.

If θ is an odd number of times of $\frac{\pi}{2}$, and $x(t) \ll \lambda$, where λ is the wavelength of light. According to the principle of small angle approximation, baseband signal can be approximated into the following equation,

$$BD(t) = \frac{4\pi x(t)}{\lambda} + \Delta\phi(t). \tag{5}$$

In this case, the optimum demodulation point will occur. When we ignore the influence of the remainder term $\Delta\phi(t)$, the baseband signal and the periodic thoracic movement displacement $x(t)$ will form a linear ratio.

When θ is an even multiple of $\frac{\pi}{2}$, baseband signal can be approximated as Equation (6):

$$BD(t) = 1 - \left[\frac{4\pi x(t)}{\lambda} + \Delta\phi(t)\right]^2. \tag{6}$$

In this case, the baseband signal and time-varying displacement cannot form a linear ratio. A null demodulation point will occur when the vibration signal and echo signal are in 0-degree phase or 180-degree phase shift. It could be solved by obtaining two signals that have a 90-degree phase difference to eliminate the disturbed redundancy. Therefore, the echo signal contains the information of respiration, heartbeat and body movement. This article designs a special circuit that could produce the non-orthogonal I/Q signals to solve this problem. And it will be introduced in next part.

III. DESIGN AND IMPLEMENTATION

This article designed and implemented an RF sensor. The block diagram is presented in Fig. 1. Parts of circuits of the sensor will be introduced in this part.

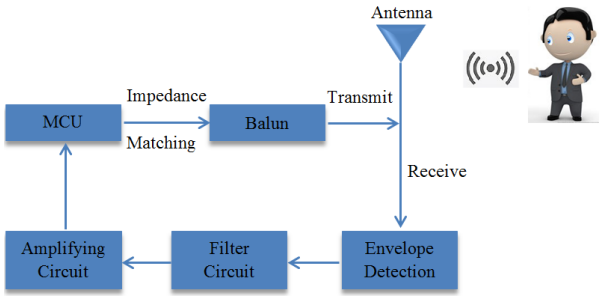

Fig. 1. Block diagram of our designed sensor.

A. Yagi antenna design

The Yagi patch antenna has a high directivity, low profile and it has attracted more interest in recent years. Considering the simple structure and high directivity, Yagi patch antenna is selected for detecting physiological parameters such as the heartbeat, respiration in daily life.

According to the principle of Yagi antenna design, a higher gain is associated with a larger size. It is balanced between the gain and the size of this sensor. The transmission distance is also taken into account. The designed Yagi antenna, which consisted of two dipole elements, a reflector and three director patch elements, is shown in Fig. 2. The length of two dipole elements is equal to the half of the wavelength. For the sake of size and universal feasibility, the antenna was designed for working at 2.4 *GHz*, which belongs to industrial scientific medical (ISM) band [18].

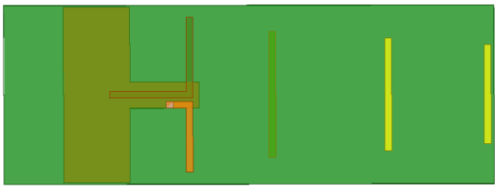

Fig. 2. The configuration designed Yagi antenna.

According to the working frequency f_0 and the speed of light C_0, we could get the wavelength in vacuum:

$$\lambda = \frac{C_0}{f_0}. \quad (7)$$

The original antenna patches are based on the FR4 (a kind of level code of fire resistant) substrate with the thickness of 1.2 *mm*. The permittivity (ε_r) of FR4 substrate is 4.4. When the electromagnetic wave transmits in the medium whose permittivity is ε_r, the speed of light will change to:

$$c = \frac{C_0}{\sqrt{\varepsilon_r}}. \quad (8)$$

Therefore, the length of the two dipole elements should be shorter than the half of the wavelength. Using electromagnetism simulation software-HFSS (Version 14.0), this article designed a Yagi patch antenna based on the FR4 substrate with the thickness of 1.2 *mm*, and size of 154.5*54 mm^2.

Compared with five or more director elements in other literature, this paper achieved the high gain of 7.7 *dB* with using three director elements, which reduced the size of Yagi antenna. A special broad-band microstrip-to-coplanar strip line (CPS) Balun structure was also designed to make the antenna's impedance equal 50 *ohm* instead of using the CPS Balun and impendence converter in the common Yagi design [19-22] as shown in Fig. 3. According to the microwave radiation principle, the currents in the two dipole elements have opposite direction and the same amplitude [23]. We designed one via hole connecting one of dipole elements with the reflector to simply the structure of antenna and reduce the size of the antenna as shown in Fig. 3 (b). The Port1 connects directly with the output of the radio frequency (RF) as the input of RF signals. Adjusting the distance of the Port2 connecting with the microstrip and the Port3 connecting with the reflector by the vial hole can change the amount of coupling between the coplanar strip lines. This paper adjusted the distance to make the currents in two dipole elements have the same amplitude.

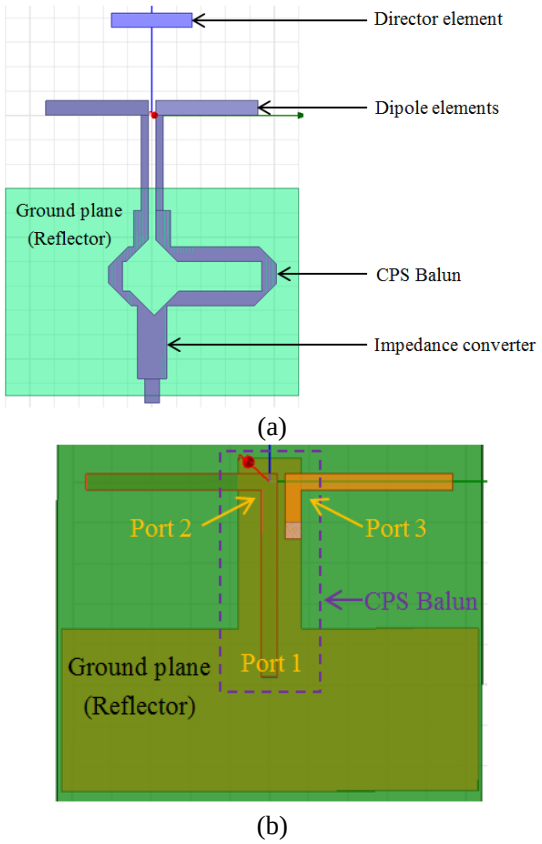

Fig. 3. Structure of Yagi antenna. (a) Structure of common Yagi antenna [19]; (b) structure of our designed Yagi antenna.

In this article, the Yagi antenna and the circuits are printed on a PCB. In order to have enough space to place the circuits, this paper increased the width of the reflector from 2 *mm* to 20 *mm*, resulting in influencing the performance of the RF sensor. For a satisfied directivity and higher gain, this paper increased the length of the reflector and reduced the distance between reflector and dipole element at the same time.

B. Circuit design

At present, an RF micro control unit (MCU) of Nordic company is employed in our sensor. The features of this MCU are low consumption and embedded

transmission protocol. The sensor was designed for working long time in our daily life, which means low power consumption. Those features are suitable for monitoring daily vital signs.

Design of high frequency circuit is different from low frequency circuit design. There might be a variety of unexpected issues emerged because of inappropriate high frequency circuit design. This sensor is an integration of antenna and circuit, which means that the circuits will be disturbed by the high frequency part. Therefore, it is of vital importance to reduce the disturbance caused by high frequency.

Considering the polarization of the Yagi antenna, the direction of current flowing on the PCB is perpendicular to the direction of microwave propagation. One of the most effective ways is Balun (balanced-to-unbalanced). Usually, the transmitter is regarded as unbalanced and the antenna is regarded as balanced. Balun is a converter to get the resistance matched. Furthermore, the standing wave will be reduced obviously by the Balun. It is represented on the MCU datasheet about how to design a Balun for this MCU. However, this paper has designed a new Balun to match our antenna. As Fig. 4 depicted, the layout of components were arranged elaborately to lower power dissipation.

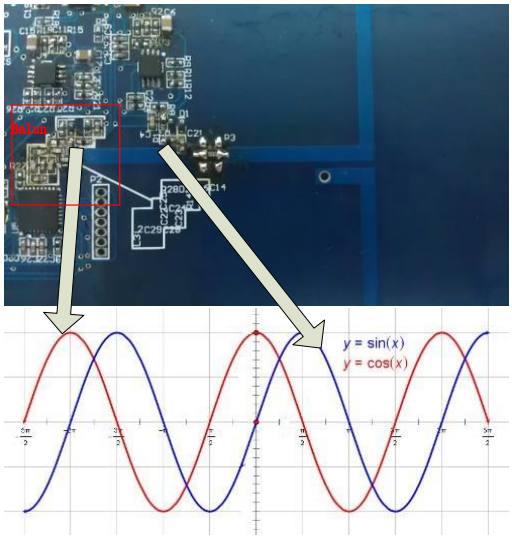

Fig. 4. Special circuits design.

As shown in Fig. 4, this paper designed a wire whose length is equal to one-eighth of the wavelength. And it was mounted between the MCU and the Yagi antenna. When the MCU transmits and receives a signal through this wire, two signals with 90-degree phase difference will be acquired at its two ends. According to the contents described in the "principle of detecting body motion by microwave" section, a new signal without the null demodulation point will be generated after reconstruction.

This paper produced RF signals by downloading program into the chip rather than producing it by some high frequency analog circuits, such as a voltage controlled oscillator (VCO) circuit, a mixers circuit in other literatures. The high frequency circuits are a Balun circuit and an envelope detection circuit, which reduce the loss of the high frequency and the influence of the circuits.

As shown in Fig. 5, the RF chip was set to transmit a pulse-square wave whose period is 10 *ms* at the carrier frequency of 2.4 *GHz*. According to the previously described, the echo signal contains some information about body movement. The envelope detection circuit can remove high frequency components and demodulate the human dynamic information of low frequency component. Then the signals were filtered and amplified. Using an analog to digital converter (ADC) converts analog signal into 8 hex decimal number coding and encodes it into a pulse by Gauss frequency shift keying (GFSK). Finally, the signal is sent at the carrier frequency of 2.4 *GHz*.

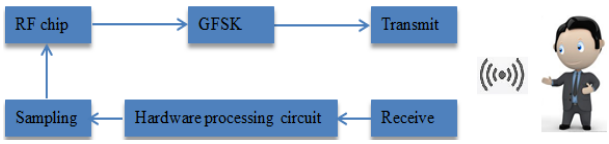

Fig. 5. Block diagram of software design.

In high frequency circuits, the phase of signal changes with the length of the wire. This article has taken advantage of this special characteristic to get two echo signals in one sensor.

C. RF sensor implementation

Well-implemented PCB antennas have similar performance with that of a ceramic antenna. However, the performance of the antenna will be changed after adding circuits to the board. In order to make it work at 2.4 *GHz* properly and have a high gain at the same time, this paper adjusted the length of dipole element and rebuilt ground for the circuits. Adding circuits to the original antenna makes the simulation more complex. The wires in these circuits are subtle and the components are different in irregularity shapes and sizes, which add a lot of burden to the simulation, especially increase the amount of calculation. However the compute capability of the computer is limited. In order to improve the simulation performance and the computational complexity meanwhile, this paper simulated the long wires, all the large size via holes and components close to the antenna. On the contrary, we ignored the influences of the rest of components and wires to simplify the model. While simulation results are slightly

affected due to simplification, so we increase the area of reflector and adjust the distance between the reflector and the dipole element. However, via holes are remained since via holes on the reflector may produce the parasitic capacitance and inductance and change the characteristic impedance, which influences the result of the RF sensor.

If the distance (D1) between dipole element and the first wave-guider is shorter than the distance (D2, D3) between the other wave-guiders, the antenna will have a higher gain. Figure 6 and Table 1 show the main parameters of the designed RF sensor.

Table 1: Main parameters of the Yagi antenna

Parameter	L1	L2	L3	L4	D1	D2	D3
Size (mm)	42.6	39.7	36.0	29.5	24.0	32.0	28.45

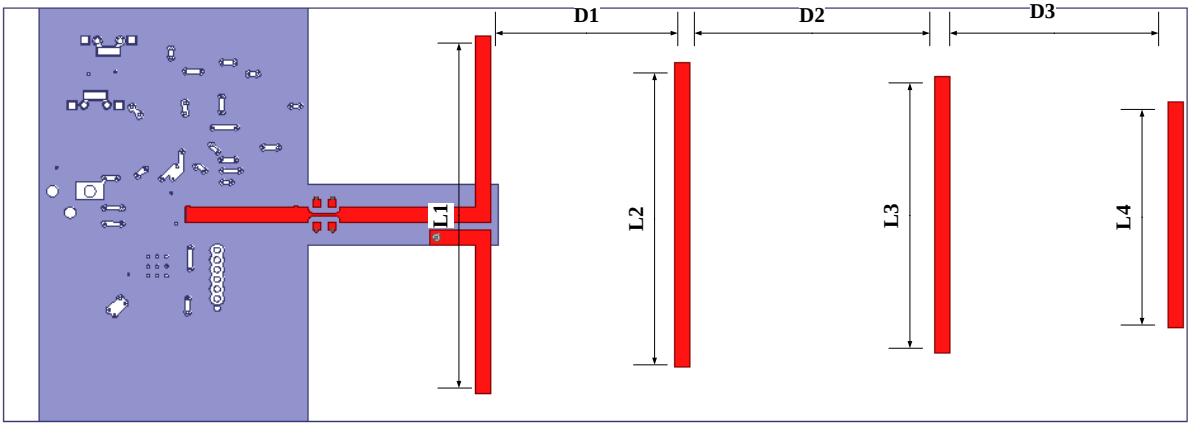

Fig. 6. Main parameters of the designed antenna and circuits.

IV. RESULTS AND DISSCUSSIONS

A. Parameter S11

When the impedance mismatches the antenna from the fed line of transmitter or receiver, the system performance will be declined due to the reflection. The sensor is an integration of the antenna and circuits, so it is important to examine the return loss of this design. Parameter S11 is a distinct factor to examine the performance of an RF component.

The HFSS solver was employed to simulate and process the data. Figure 7 (a) shows the simulated S11 parameters at different frequencies with a single Yagi antenna. The value of S11 is -15.30 *dB* in 2.4 *GHz* and resonance point is placed exactly at 2.4 *GHz* as demonstrated. This value is a considerable result which means most of the electromagneticwave is transmitted by designed antenna and only few are returned. The results demonstrate that the Yagi patch antenna has a nice match in 50 *Ω*.

Figure 7 (b) shows the experimental S11 results of designed sensor measured by a network analyzer. These are the final results after some experiments. By analyzing the simulated results, some improvements were achieved. For instance, the resonance point was deviated from 2.4 *GHz* thus this article enlarged the area of the ground to make the sensor working at the frequency of 2.4 *GHz* properly. Table 2 shows the return loss (RL) of the original antenna and the integrate system at different frequencies.

Table 2: Return loss of simulation and experiment.

Frequency (*GHz*)	2.400	2.450	2.485
RL of integration (*dB*)	-15.30	-10.32	-7.21
RL of real sensor (*dB*)	-22.77	-14.72	-10.27

From Table 2, the return loss of the sensor evidently shows our improvements' effect. At the frequency of 2.4 *GHz*, the return loss of the sensor reaches -22.77 *dB*. The experimental results are better than simulated results after our adjustment, although the resonance frequency of experiments is not exactly at 2.4 *GHz*.

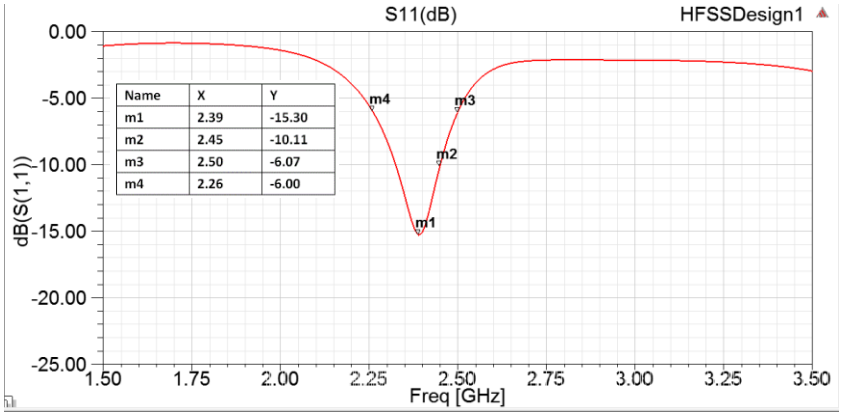

(a)

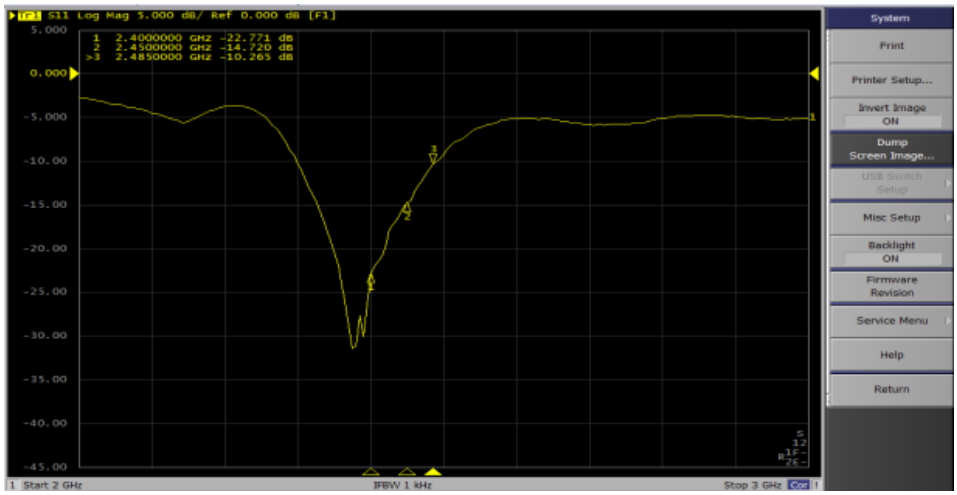

(b)

Fig. 7. S11 of simulation and experimental results. (a) Simulated results; (b) the experimental result.

B. Radiation pattern

Radiation pattern is another indicator which can depict the performance of an antenna. The results about radiation pattern of sensor were obtained by using software-HFSS to get the simulated results. And the experimental results were obtained at a professional chamber for microwave measurement. Figure 8 shows the environment of the experiment.

Figure 9 (a) shows the simulated result about co-polarization at electricfield plane from the sensor. It can be found that there is a maximum gain of 7.71 *dB* in the front. And the directionality which concentrates most power in the front and is satisfactory for detecting physiological parameters.

Considering the different methods and standard of measurement between the real experiment and HFSS, Fig. 9 (b) shows the experimental result about co-polarization at electricfield plane from the sensor.

The parameters of the original antenna were settled after simulating, however, the performance of the antenna was changed totally after adding circuits to it. And the practical implementation is performed with some uncertainty factors, such as the wires, components and soldering, may influence the antenna profoundly. This paper took some adjustments to improve the performance by adjusting the Balun circuit and other improvements as it is said in the circuit design section. The S11 parameter was placed at the first position thus there will be a compromise about radiation pattern.

Fig. 8. Experimental environment of our testing.

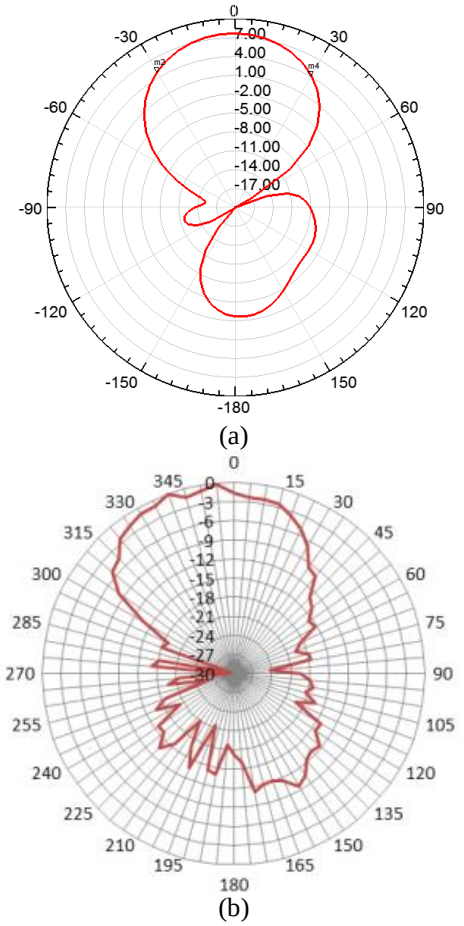

Fig. 9. Radiation pattern of the sensor. (a) Simulated result; (b) experimental result.

The simulated result and experiment result both have a huge front lobe. That means the sensor could concentrate more power on the front and will promote sensitivity effectively. The back lobe of the sensor is larger than simulated result, which might be caused by electronic components. The result is under our consideration and acceptability for monitoring vital signs. Figure 10 shows the designed RF sensor.

Fig. 10. Our designed RF sensor.

C. Experiment results

All the results were obtained by the sensor directly and transmitted to PC with a receiver. The performances of designed RF sensor are compared with the pulse sensor, and respiration sensor as a reference. Figure 11 shows the signals collected by RF sensor without any processing. The signals were collected at the distance of 20 *cm* from Yagi antenna with objects facing towards the Yagi antenna and wearing the pulse sensor and respiration sensor at the same time. The duration of the data collection was 60 seconds for each dataset. Figure 11 (a) shows the original signal collected by designed RF sensor. According to the Doppler principle, echo signal consists of information on heartbeat, respiration and body movement as shown in the Fig. 11 (b).

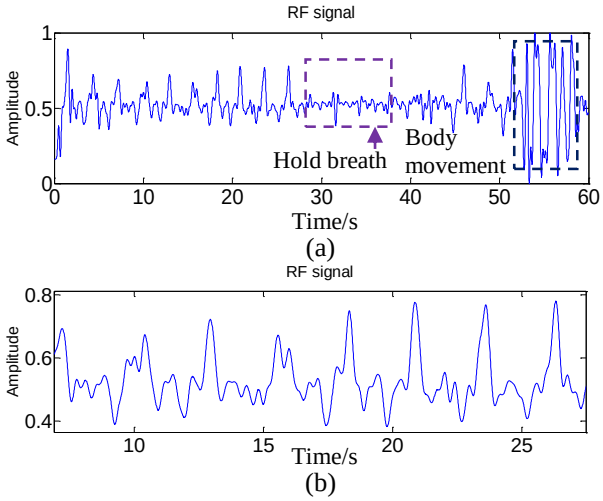

Fig. 11. Signals collected by RF sensor. (a) Original signals collected by RF sensor; (b) local amplification of original information.

The extraction of heartbeat and respiration is achieved by digital filter to filter some noise and wavelet transform. Comparing with the signals collected by the pulse sensor and respiration sensor, our designed RF sensor is able to monitor the vital signs. Figure 12 shows the respiration signal and heartbeat signal collected by the respiration sensor (Fig. 12 (a) TOP) and heartbeat sensor (Fig. 12 (b) TOP) as a reference signal in comparison with the signal collected by signals collected by RF sensor. It is notable that the heartbeat signal and respiration signal obtained from RF sensor closely agree with that of the reference.

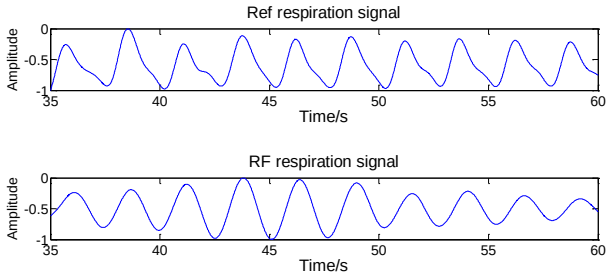

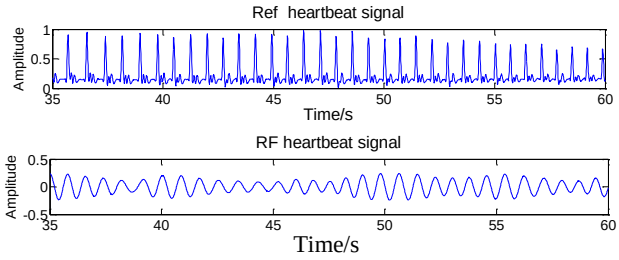

(b)

Fig. 12. Signals acquired by RF sensor, respiration sensor and pulse sensor. (a) Respiration from respiration sensor and RF sensor; (b) heartbeat signal from pulse sensor and RF sensor.

V. CONCLUSIONS

A single-channel non-orthogonal I/Q RF sensor was designed for non-contact monitoring of vital signs. The maximum gain of our designed sensor in the front is 7.7 *dB*. And the chip separates the transmitted signals and received signals by our designed program. Also, the directionality of the antenna is satisfactory. After simulation, experiment and compared with the respiration, heartbeat sensor, it was validated that the sensor could monitor the respiration, heartbeat and body movements accurately.

ACKNOWLEDGMENTS

This work is supported by the National Natural Science Foundation of China (No. 61374015, No. 61202258), the Ph.D. Programs Foundation of Ministry of Education of China (No. 20110042120037), the Liaoning Provincial Natural Science Foundation of China (No. 201102067) and the Fundamental Research Funds for the Central Universities (No. N110219001).

REFERENCES

[1] M. K Rajagopal and E. Rodriguez-Villegas, "Towards wearable sleep diagnostic systems for point-of-care applications," *IEEE Point-of-Care Healthcare Technologies*, vol. 25, pp. 26-29, 2013.

[2] Y. Nijsure and W. P. Tay, "An impulse radio ultra-wideband system for contactless noninvasive respiratory monitoring," *IEEE Transactions on Biomedical Engineering*, vol. 60, pp. 1059-1517, 2013.

[3] C. Hoffman, D. Rice, et al., "Persons with chronic conditions: their prevalence and costs," *Journal of the American Medical Association*, vol. 276, pp. 1473-1479, 1996.

[4] Y. Yan, C. Li, et al., "Verification of a non-contact vital sign monitoring system using an infant simulator," *2009 Annual International Conference of the IEEE Engineering in Medicine and Biology Society*, pp. 4836-4839, 2009.

[5] J. C. Lin, "Microwave sensing of physiological movement and volume change: A review," *Bioelectromagnetics*, vol. 13, pp. 557-565, 1992.

[6] D. Zito, D. Pepe, and M. Mincica, et al., "Wearable system-on-a-chip UWB radar for contact-less cardiopulmonary monitoring: Present status," *Conf. Proc. IEEE Eng. Med. Bio. Soc. 2008*, vol. 14, pp. 5274-5277, 2008.

[7] M. Mincica, D. Pepe, et al., "Enabling technology for heart health wireless assistance," *The 12th IEEE Int. Conf. on e-Health Networking Applications and Services*, pp. 36-42, 2010.

[8] A. Droitcour, V. Lubecke, et al., "A microwave radio for Doppler radar sensing of vital signs," *IEEE MTT-S Int. Microw. Symp. Digest*, vol. 5, pp. 175-178, 2001.

[9] A. D. Droitcour, O. Boric-Lubecke, et al., "Range correlation and I/Q performance benefits in single-chip silicon Doppler radars for non-contact cardiopulmonary monitoring," *IEEE Transactions on Microwave Theory and Techniques*, vol. 52, pp. 838-848, 2004.

[10] V. Vasu, C. Heneghan, et al., "Signal processing methods for non-contact cardiac detection using Doppler radar," *IEEE Workshop on Signal Processing Systems*, pp. 368-373, 2010.

[11] C. Li and J. Lin, "Non-contact measurement of periodic movements by a 22-40 GHz radar sensor using nonlinear phase modulation," *IEEE/MTT-S International Microwave Symposium*, pp. 579-582, 2007.

[12] Y. Xiao, C. Li, et al., "Accuracy of a low-power Ka-band non-contact heartbeat detector measured from four sides of a human body," *IEEE MTT-S International Microwave Symposium Digest*, pp. 1576-1579, 2006.

[13] D. Girbau, A. Lazaro, et al., "Remote sensing of vital signs using a Doppler radar and diversity to overcome null detection," *IEEE Sensors Journal*, vol. 12, pp. 512-518, 2012.

[14] S. A. Bokhari, J. F. Zuercher, et al., "A small micro-strip patch antenna with a convenient tuning option," *IEEE Transactions on Antennas and Propagation*, vol. 44, pp. 1521-1528, 1996.

[15] C. Li, J. Cummings, et al., "Radar remote monitoring of vital signs - from science fiction to reality," *IEEE Microwave Magazine*, vol. 10, pp. 47-56, 2009.

[16] H. J. Kim, K. H. Kim, et al., "Measurement of human heartbeat and respiration signals using phase detection radar," *Review of Scientific Instruments*, vol. 78, pp. 104703, 2007.

[17] A. D. Droitcour, O. Boric-Lubecke, et al., "Signal-to-noise ratio in Doppler radar system for heart and respiratory rate measurements," *IEEE Transactions on Microwave Theory and Techniques*, vol. 57, pp.

2498-2507, 2009.
[18] J. Zhao, L. Xu, et al., "Analysis and design of a printed Yagi antenna working at the frequency of 2.4 GHz for monitoring physiological parameters," *The 11th World Congress on Intelligent Control and Automation*, pp. 543-547, 2014.
[19] W. R. Deal, N. Kaneda, et al., "A new quasi-Yagi antenna for planar active antenna arrays," *IEEE Transactions on Microwave Theory and Techniques*, vol. 48, pp. 910-918, 2000.
[20] A. Abbosh, "Ultra-wideband quasi-Yagi antenna using dual resonant driver and integrated Balun of stepped impedance coupled structure," *IEEE Transactions on Antenna and Propagation*, vol. 61, pp. 3885-3888, 2013.
[21] Y. Chen, C. Zhang, et al., "Modified quasi-Yagi antenna," *Modern Radar*, vol. 31, pp. 60-62, 2009.
[22] G. Ni, W. Ni, et al., "Design of planar UWB quasi-Yagi microstip antenna," *Modern Radar*, vol. 35, pp. 48-51, 2013.
[23] J. Venkatesan, "Novel version of the double-Y Balun: Microstrip to coplanar strip transition," *IEEE Antennas and Wireless Propagation Letters*, vol. 5, pp. 172-174, 2006.

H. R. Bo received the B.S. degree in Biomedical Engineering from Northeastern University, Shenyang, China, 2014, and is currently working toward the M.S. degree at the Northeastern University, Shenyang, China.

His research interests include antenna structures and arrays, digital signal processing and electronic circuits.

L. S. Xu (SM'15) received the B.S. degree in Electrical Power System Automation, the M.S. degree in Mechanical Electronics, and the Ph.D. degree in Computer Science and Technology from Harbin Institute of Technology, Harbin, China, in 1998, 2000 and 2006, respectively.

His current research interests include nonlinear medical signal processing, computational electromagnetic simulation, medical imaging, and pattern recognition.